University of the Basque Country

PhD Thesis - 2016

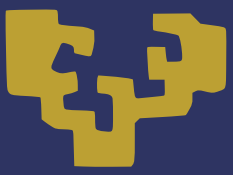

LOWER BOUNDS ON QUANTUM METROLOGICAL PRECISION

Author:
Iagoba Apellaniz

Director:
Géza Tóth

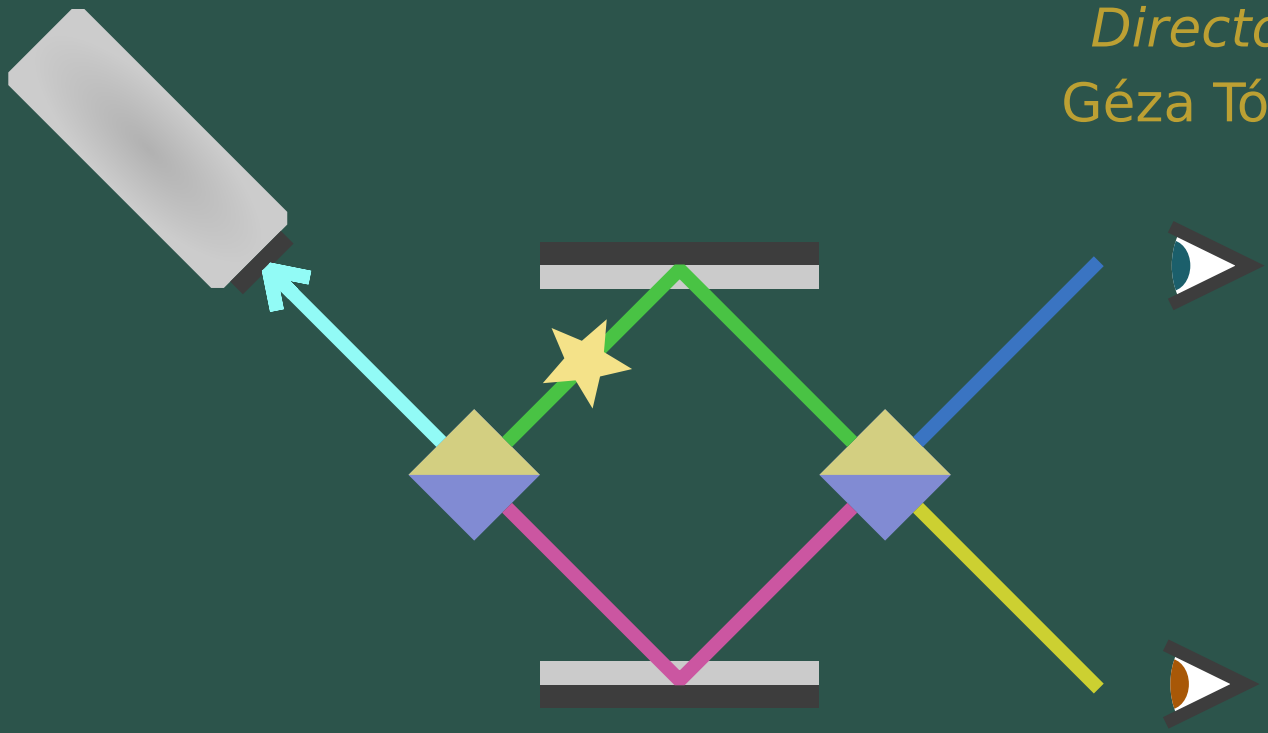

This document was generated with the 2014 distribution of LaTeX.

Prologue

This work is part of doctoral project which I started on the sumer of 2013. This work collects almost all the research I have done on those previous years. I try to be as clear as possible, writing from the very basics concepts of modern Quantum Physics until the most recent results on Quantum Metrology and Quantum Information in a clear and concise way, such that it is understandable for a more general public.

The research work I collect in this thesis was done in collaboration with members of the group I belong to. Even if not all of them are at the present day investigating on our group, the collaborators namely were Dr. Philipp Hyllus, Dr. Giuseppe Vitagliano, Dr. Iñigo Urizar-Lanz, Dr. Zóltan Zínboras, Dr. Matthias Kleinmann and Prof. Géza Tóth. Apart from the group GEDENPQOT, based on Bilbao, this thesis also collects some works done in collaboration with the group Theoretical Quantum Optics lead by Prof. Otfried Gühne of the University of Siegen, in Germany, and the group of Prof. Carsten Klempt at the Universitu of Hannover, in Germany too.

Publications

Iagoba Apellaniz *et al*, *New J. Phys.* **17** 083027 (2015)
Detecting metrologically useful entanglement in the vicinity of Dicke states

Géza Tóth and Iagoba Apellaniz, *J. Phys. A: Math. Theor.* **47** 424006 (2014)
Quantum metrology from a quantum information science prespective

Preprints

Out of the scope of this thesis

Giuseppe Vitagliano *et al* 2014 *Phys. Rev. A* **89** 032307
Spin squeezing and entanglement for an arbitrary spin

Contents

Tables, figures and abbreviations

Abbreviations

SLD – Symmetric logarithmic derivative
QFI – Quantum Fisher information

Figures

Tables

SLD – Symmetric logarithmic derivative
QFI – Quantum Fisher information

University of the Basque Country

PhD Thesis

Lower bounds on quantum metrological precision

Author:
M. Sc. Iagoba Apellaniz

Director:
Prof. Géza Tóth

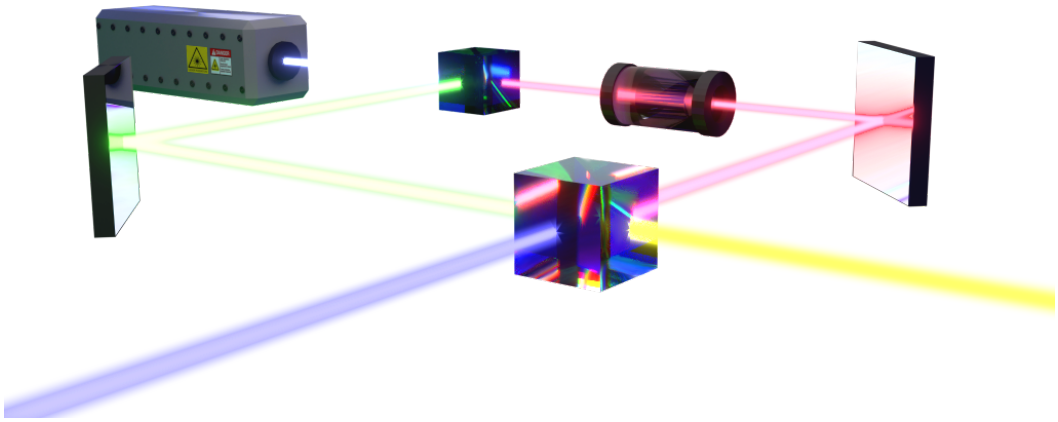

July 13, 2016

To my parents, my family

and to all the people

I have had around me those years.

Acknowledgments

I want to thank the people that support me in this endeavor especially my office and discussion mates and my director Géza Tóth for without whom my work would not be even started. I also want to thank more people especially those from the theoretical physics department of the University of the Basque Country and the unique very especial group for me from the Theoretical Quantum Optics group at the University of Siegen. I would really like to mention the names of all of them but I think it would be quite heavy for the average reader of this thesis. Thank you guys! Also I want to thank people from the group QSTAR at Florence, Italy.

On the other hand I also felt very comfortable at my university, the University of the Basque Country, but I want to thank especially the people that make me grow in all ways as person.

1 Introduction

In the recent years...

The figure of merit for the precision is the inverse of the variance normalized with the number of particles, $(\Delta\Theta)^{-2}/N$. It has the following properties:

(i) The bigger it is the bigger is the precision

(ii) It is normalized so for the best separable state it is 1. For greater values than 1 it would be a non-classical sign.

SQL

$$(\Delta\Theta)^{-2} \leq N \tag{1.1}$$

HL

$$(\Delta\Theta)^{-2} \leq N^2 \tag{1.2}$$

This thesis consists of 4 well differentiated parts, apart from the current introduction, on which different topics are developed. In the first part, we will introduce the reader onto the research field

of quantum metrology.

Brief comments on the notation: c_Θ and s_Θ stand for $\cos(\Theta)$ and $\sin(\Theta)$ trigonometric functions respectively. We will skip on writing the tensor-product notation $\otimes$ if it is not strictly necessary for the correct comprehension of the text.

2 Background on Quantum Metrology

Metrology, as the science of measuring, has played an essential role for the development of the technology as we know it today. It studies several aspects of the estimation process, such as which strategy to follow in order to improve the precision of an estimation. One of the most important figure of merit in this context is the achievable precision for a given system, independently of the strategy. We will show how to characterize it in the subsequents sections. And we will show as well different strategies to achieve the desired results. The metrology science also covers from the design aspects of a precise measuring device, until the most basic concepts of nature which lead in ultimate instance to the better understanding of the whole process.

In this sense, with the discovery of the Quantum Physics and the development of Quantum Mechanics, new doors for advances in metrology were open on the earlies decades of the 19th century. Later on, the Quantum Theory lead to the so-called field of Quantum Information which merges the notions of the theory of information and computer science, among others subfields, with the quantum mechanics. The role of the so-named entanglement, an exclusive feature of Quantum Mechanics, is essential in this context. Its complete understanding has integrated efforts of many researches world wide. Said this, the entanglement also is in the center of theoretical concepts included in Quantum Metrology.

On the other hand and with the aim of interpreting raw data, there are the statistics, without which

Tree #	1	2	3	4	5	6	7	8	9	10	11	12	13	14	15	16	17	18
Heights (m)	6	7	5	7	2	11	7	4	7	2	7	7	5	5	5	8	3	10

Table 2.1: A set of values for the heights of 18 trees. All measurements were rounded to integers for simplicity.

many descriptions of the actual and past physical findings would lack of the rigorous interpretation needed for the complexity of data samples.

2.1 Background on statistics and the theory of estimation

The main mathematical tools used by the metrology science belong to statistics. Moreover we are also interested on estimation theory. The statistics main characteristic is that makes the raw data under consideration comprehensible. The data can be anything, from a set of different heights of a basketball team, to the outcomes of a coin toss or the ages of a hundred students or even the outcomes of a thousand times repeated measurement of the electric field at some spatial point. The aim of this section is to give the reader sufficient material to follow this thesis and make it comprehensible from the beginning.

2.1.1 Data samples, average and variance

As we mentioned above, everything in statistics starts with a data sample. A data sample is defined as a set of values, we will restrict ourselves to quantitative values for simplicity, representing some magnitude. So, in our framework such a set can be written as $X = \{x_i\}_{i=1}^{M}$, where all M values are collected. An illustrative example with 18 heights of different trees is shown on the Table 2.1. It is worth to notice that this data sample represents a continuous variable, the height of some trees, while we have grouped more than a single instances into integer values. If we would use more decimals to describe the data probably all values would have been different among each other. This discussion is not so essential when discrete outcomes are analyzed

This picture can be extend to more outcomes coming from a single *event* or measure. For instance, a second value such as the width of the tree could be attached to each height on the previous example. This way we have opened our approach for higher dimensional data samples that can be described as a set of M outcomes with more than a single value each, $(X, Y, \dots) = \{x_i, y_i, \dots\}_{i=1}^{M}$.

Average

With this data at hand one of the first questions arises is whether the values of X are around some mean value. If one tries to address this question one of the first approaches can be computed is the *arithmetic average* of the set X, namely,

$$\mathrm{E}[X] := \frac{1}{M}\sum_{i=1}^{M} x_i. \tag{2.1}$$

Apart from the arithmetic average there are other types of averages such as the geometric mean, the root mean square or the harmonic mean, etc. For more information see those some of those fascinating works about the statistics [XXX]. For us and for the complete understanding of this thesis will be enough with the arithmetic average.

Let us take the previous example of the trees and compute the average. In this case the data sample is constituted by positive integer values for simplicity. The average of the data sample is straight forward $\mathrm{E}[X] = \frac{1}{18}\sum_{i=1}^{18} x_i = 6\mathrm{m}$.

For the extension to the case of higher dimensional data samples one can say that each kind of outcome the average can be computed in a seamless way, $\mathrm{E}[Y] = \frac{1}{M}\sum_{i=1}^{M} y_i$ and so on.

Variance

The second quantity one can compute is how spread the data is. This is usually done first subtracting the average to all values on the data sample, then squaring them, so the sign of the result is lost, and finally one averages over all the resulting set. This quantity is called the *variance* of the sample and it is written as follows,

$$\mathrm{V}[X] := \mathrm{E}\left[(X - \mathrm{E}[X])^2\right], \tag{2.2}$$

where X can be seen as a vector and when subtracting the scalar $\mathrm{E}[X]$ and X^2 stands for the elements wise squared of X, namely $X^2 := \{x_i^2\}_{i=1}^{M}$. The variance can also be written alternatively as $\mathrm{V}[X] = \mathrm{E}[X^2] - \mathrm{E}[X]^2$. The definition of the *standard deviation* follows directly from the variance, $\sigma_X = \sqrt{\mathrm{V}[X]}$. Many quantities on statistics require operations like the one described right before. This can be generalised again for more than one kind of outcome as it was done with the average.

Now let us see how result the variance for the example of the Table 2.1. In this case the variance would be the following, $\mathrm{V}[X] = \frac{1}{18}\sum_{i=1}^{18} x_i^2 - 6^2\mathrm{m}^2 = 5.5\bar{5}\mathrm{m}^2$.

To summarise and using the standard deviation, one can say now about the original distribution that most values are around 6m with a deviation of 2.357m. Of course, some values are outside this

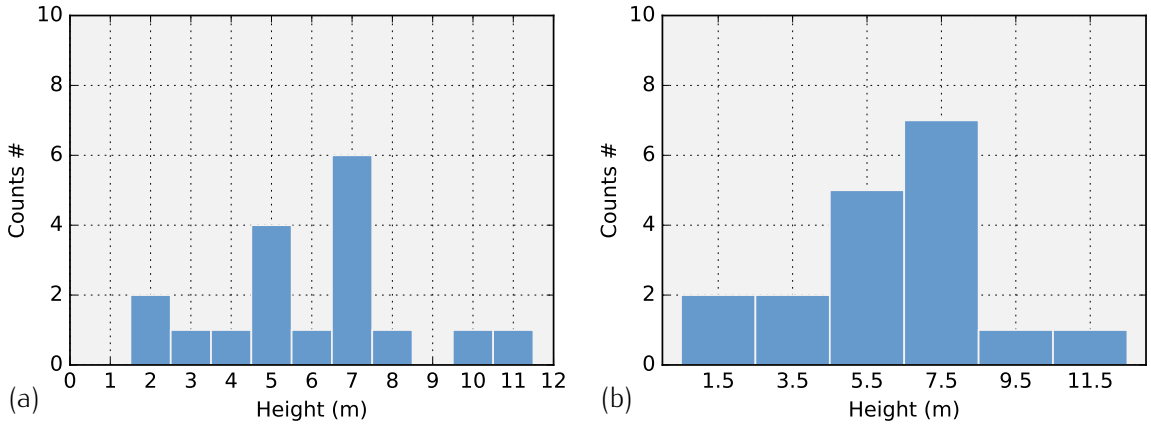

Figure 2.1: (a) p_i for different values of i. All bars have width as 1, so it is drawn how many times each data value appears on the data sample. The width of the bars is called *bin*, and it can change so the bars would represent a wider range of values. (b) Yo can see the same data represented in this case by a histogram with the bin size equal to 2. To produce this histogram we have summed 2 adjacent p_i values starting from $p_1 + p_2$, $p_3 + p_4$ and so on. Those new bars we have chosen to represent a value in between, for instance $(3 + 4)/2 = 3.5$ and so on.

range, but nevertheless the description is quite accurate, note that 12 values from 18 are inside the range 6m $\pm$ 2.357m.

Histograms

At this point we introduce the *histograms* and with that, first, the *distribution function* of the data sample. Returning to the example of the Table 2.1, one may notice that the value 7m is repeated 6 times, as the value 5m is 4 times and so on. This is represented with the distribution function p_i, which in this case is for discrete values of the outcomes but which can be generalized for continuous variables as we will see later. This function takes the value of how many times the outcome i has appeared on the data sample. Let us plot the distribution function, see Figure 3.3.

Now some question arises immediately: How this is fully connected with the previous picture? How can one compute the average and other interesting quantities? The answer is simple but it has to be considered carefully. First of all, notice that p_i is defined for all the natural numbers including zero, see that in the example of the trees p_9 equals zero, so it can be extended for other heights too setting them to zero. This will depend on the physical property that our data sample represents but in this case it is the height of some trees, so the values cannot be negative. Second, notice that the sum of all the repetitions, all the values of p_i, is exactly 18 the number of data samples in the set. So we have that $M = \sum_{i=0}^{\infty} p_i$. Now we can formulate the ensemble average as $\mathrm{E}[X] = \sum_{i=0}^{\infty} p_i i / \sum_{j=0}^{\infty} p_j$. The variance and with this the standard deviation immediately follow this approach. It is convenient

to notice that the total measurement outcomes has not contribute anything but to normalize the quantities.

We can now without losing generality redefine the distribution function to be the number of repetitions corresponding to the variable divided by the total outcomes, in this case M. It would have the same properties of a probability distribution function (PDF). For instance, now we have that the sum of all p_i-s equal to one, $\sum_{i=0}^{\infty} p_i = 1$, and the average is directly obtained by computing $\mathrm{E}[X] = \sum_{i=0}^{\infty} p_i i$. This is the approach we will follow to represent data samples. The variance and other quantities also are simpler in this way.

2.1.2 Probabilities and frecuentist vs. bayesian approach

Let us talk now about probabilities. The notion of the probability comes, [XXX]. In our contest we will define the probability in the following way. Imagine we have an unknown data sample, let say X, from which we randomly choose one of the data values. The probability to obtain a random variable x is given by the parent distribution function divided by the population number M.

We can estimate the average height of the trees of that forest.

histogram

estimator

Explain how for bigger bin sizes, the error for higher statistical moments increases.

MLH

CLT

2.1.3 Estimators, Fisher information

Error propagation formula.

2.2 Quantum Mechanics from metrology perspective

The ubiquitous probabilistic nature of quantum mechanics forces all the community to know some basics on probability and statistics.

The quantum state, multi-particle state, entanglement

A *system state* in Quantum Mechanics lives on a Hilbert space, $\mathcal{H}$. The system state, ρ, has the following properties:

i) It is Hermitian, so it is invariant under the complex transposition, $\rho = \rho^\dagger$.

ii) Its trace is equal to one, $\mathrm{tr}(\rho) = 1$.

iii) It is positive semi-definite, *i.e.*, all its eigenvalues are bigger or equal to zero, $\rho = \sum_\lambda p_\lambda \Pi_\lambda$[1] where $p_\lambda \geq 0$ are the scalar eigenvalues. It follows that $\sum_\lambda p_\lambda = 1$.

iv) If all p_λ are zero except one, the state is a pure state, $\rho = \Pi_\lambda$.

v) It follows that the quantum states form a convex set where the extremal points are pure states.

The composite system of N different parties lives on $\mathcal{H} = \mathcal{H}^{(1)} \otimes \mathcal{H}^{(2)} \otimes \cdots \otimes \mathcal{H}^{(N)}$ or for short $\mathcal{H} = \bigotimes_{i=1}^{N} \mathcal{H}^{(i)}$, where $\otimes$ stands for a tensor product like construction. For instance, this composite Hilbert space could be used to represent a many-particle system, in this case N particles. A *separable* state on this Hilbert space can be described in the following way,

$$\rho = \sum_i p_i \rho_i^{(1)} \otimes \rho_i^{(2)} \otimes \cdots \otimes \rho_i^{(N)}, \tag{2.3}$$

where p_i are convex weights that sum to one and are equal or bigger than zero. If not the state is said to be *entangled*.

Angular momentum operators. The angular momentum algebra comes

Entanglement cannot be described classically.

Evolution

Unitary evolution

Markov

Limblad

Measurements (POVM)

Quantum Information

[1] $\rho = \sum_\lambda p_\lambda \Pi_\lambda$ is the eigen-representation of the state, where Π_λ are the eigenstates defined on $\mathcal{H}$ too. They are as many as the dimension, d, of the Hilbert space. They are orthonormal under the product defined on such Hilbert space $\mathcal{H}$, *i.e.*, $\mathrm{tr}(\Pi_\lambda \Pi_{\lambda'}) = \delta_{\lambda,\lambda'}$. Nevertheless, there is a extended discussion when Hilbert space is defined for continuous variables, see [XXX].

2.3 Quantum Metrology

The evolution of a quantum state can be used to infer on some hidden parameter. The estimation theory applied to the intrinsic statistical nature of a quantum states has lead to the the formulation of Quantum Metrology as an important subfield. Merging the probabilistic features of quantum mechanics and the estimation theory is not trivial. Nevertheless, starting from the pioneering works of Wotters, Braunstein and some other I probably forgot to mention [XXX] were the statistical distance of neighbor states is studied we have lead to amazing results which today drive many experiments and technology. From the works of Giovannetti et al and Paris on the middle of the last decade fundamental concepts arose, for example the figure of merit quantum Fisher information or the Heisenberg limit. In this section we will highlight the most important aspects of this field and with this we will conclude this introductory chapter.

The error propagation formula for an estimation of Θ based on the observable O.

$$(\Delta\Theta)^2 \geq \frac{(\Delta O)^2}{|\partial_\Theta \langle O \rangle|^2} \tag{2.4}$$

2.3.1 Quantum Magnetometry

One of the most basic tasks of Quantum Metrology is to address the precision of estimating the magnetic field strength, namely B, of an unknown external magnetic field. In this section we will assume that the magnetic field is homogeneous on the position space. To consider more advanced situations on which the magnetic field changes linearly with the position, see chapter [XXX]. With the aim of estimating the strength of the magnetic field, a prove state is used in order to interact with it, coupling the magnetic moment of the state and the field itself. After some time, the state has evolved. Finally, measuring how the state has changed one would be able to infer on the strength of the magnetic field, basically proportional to the change on the state.

In general, we will say that the magnetic moments of the states come exclusively from the spin angular momentum, neglecting any possible contribution from the orbital angular momentum. This way the physics is simpler. This is justified in the sense that most of the recent experiments on this context have been carried out with ion-traps, BECs or at most cold atomic ensembles, which have indeed a negligible orbital angular momentum.

Beside this considerations, the interaction Hamiltonian can be written as,

$$H = -\boldsymbol{\mu} \cdot \boldsymbol{B} \tag{2.5}$$

up to some constant factor. Now in the simplest case we will choose the magnetic field to be pointing to some fixed direction, for instance, the Oz direction. So the magnetic field vector can be written as $B = B\boldsymbol{k}$, where $\boldsymbol{k}$ is the unitary vector pointing to the Oz direction. This way estimation problem is much more simple, since one has not to determine the direction of the magnetic field.

The magnetic moment of the system is proportional to the spin angular momentum, $\boldsymbol{\mu} = -\mu_B g_s \hbar^{-1} \boldsymbol{J}$, where μ_B and g_s are the Bohr magneton and anomalous gyromagnetic factor respectively. Finally, one can rewrite the interaction Hamiltonian as,

$$H = \gamma B J_z \tag{2.6}$$

where $\gamma = \mu_B g_s \hbar^{-1}$ and we have used the fact that $\boldsymbol{J} \cdot \boldsymbol{k} = J_z$. Finally, the unitary operator leading the evolution of the system can be written as,

$$U = \exp(-i\Theta J_z), \tag{2.7}$$

where the magnetic field strength is encoded into the variable $\Theta = -\mu_B g_s t B/\hbar$. Here μ_B stand for the Magneton of Bhor and g_s for the giro-magnetic constant for the spin angular momentum, and t is the time spent on the evolution.

3 Metrology in the vicinity of Dicke states

In this chapter we will present recent results regarding the metrological usefulness of a family of unpolarised states. Such states can be used as prove states to estimate the homogeneous magnetic field strength, see Section 2.3.1 for refeneces about magnetometry. It turns out that those unpolarised states are the only ones that can bite the Heisenberg limit, as it was shown on the Section [XXX]. Hence, those states have attracted the interest of the community.

One of the figures of merit of this such unpolarized, but still useful states is the so-called unpolarized Dicke state [XXX], which consists of, on its Oz-axis representation, an equal number of qubits pointing up and pointing down while the whole state is at the same time symmetrised. It can be written as follows,

$$|\mathrm{D}_N^0\rangle \equiv |\mathrm{D}_N\rangle := \binom{N}{N/2}^{-\frac{1}{2}} \sum_{k\in\sigma_s} P_k \left(|1\rangle^{\otimes N/2}|0\rangle^{\otimes N/2}\right), \tag{3.1}$$

where k are elements of the set of all possible unique permutations of N elements of 2 kinds, σ_s. This state is also called twin-fock state on different contexts. Such state is known to be highly entangled [XXX] and to reach Heisenberg scaling when used in magnetometry. For these and other reasons unpolarised Dicke states have been created in photonic systems [XXX], in cold-gases [XXX]

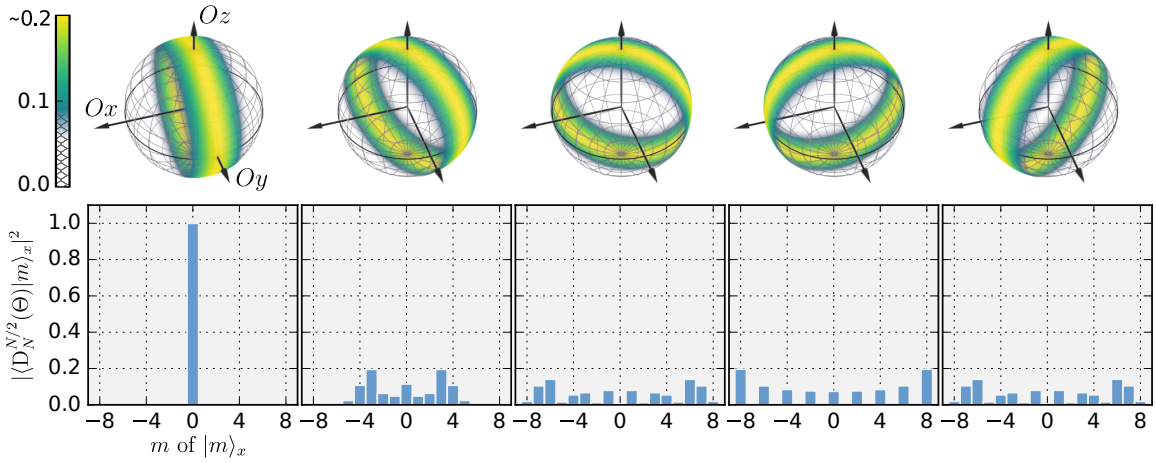

Figure 3.1: Secuence of the evolution of an unpolarized Dicke state of 16 qubits for $\Theta = \{i\pi/6\}_{i=0}^{4}$. Bloch spheres representing the Hirusi distribution of the state, and below PDF of the J_x POVM for each step of the secuence

and recently in trapped ions [XXX].

The symmetric subspace of N spin-$\frac{1}{2}$ particles is decomposed in $N+1$ orthonormal states, see Appendix B.2 for more details on how such subspaces behave even for different spins. Indeed, the subspace can be seen as a single spin-$\frac{N}{2}$ particle.

One of the most particular features this state has is that since it is a eigenstate of the collective operator J_z with corresponding eigenvalue equal to zero. At the same time, it lives on the subspace where the collective total spin is maximum, *i.e.*, $\langle \boldsymbol{J}^2 \rangle = N(N+2)/4$. Thus, with this together with the fact that the state is unpolarised, it turns that it must have a very large uncertainty for the collective spin operators perpendicular to J_z, namely J_x and J_y.

3.1 Unpolarised states for magnetometry

Having unpolarised states for magnetometry has been shown useful in Section XX. While the quantum Fisher information would give directly the performance one state would have, this is not feasible in general because a complete knowledge of the state is needed to compute such value. On the other hand, we can use the error propagation formula Equation (XX) to obtain a bound on the precision. As one can see on the Figure 4.6 a pure Dicke state is rotated along the Oz-axis. Say that in this case the initial state is an unpolarised Dicke state of aligned with the Ox-axis.

The state initially is an eigenstate of the J_x^k operators for $\forall k \in [1, \infty]$. Another feature of the sequence is that $\langle J_l \rangle = 0$ for $\forall l \in x, y, z$. It turns out that measuring the evolution of the second

statistical moment of J_x is one of the ways to go. It will start having value equal to zero for the pure unpolarized Dicke state, and rapidly will increase its value as it can be seen on the Figure 4.6. Another heuristic observation is that for $\Theta = \pi/2$ the value of $\langle J_x^2 \rangle$ will be at its maximum been it proportional to $\langle \boldsymbol{J}^2 \rangle$ so to N^2. Hence, the change on the second moment over the phase shift must be in this case proportional to N^2. From this and for those states, we lead to the conclusion that one only needs to measure the second moment of the collective spin J_x to observe precisions that scale with the Heisenberg limit. In the following equation we show the error propagation formula that will give us the obtained precision,

$$(\Delta\Theta)^2 = \frac{(\Delta J_x^2)^2}{|\partial_\Theta \langle J_x \rangle|^2}. \tag{3.2}$$

3.2 Evolution of the expectation values

With the aim of computing the precision, Equation (3.2), we will compute the dependence on Θ of the expectation value of the operator J_x and higher order moments. For that first of all we will move onto the Heisenberg picture where the operators evolve in time while the state remains the same. The operator J_x can be written a a function of Θ the following way,

$$J_x(\Theta) = e^{i\Theta J_z} J_x(0) e^{-i\Theta J_z} = J_x(0)\mathrm{c}_\Theta - J_y(0)\mathrm{s}_\Theta, \tag{3.3}$$

where $J_l(0)$ for $\forall l$ are the collective angular momentum operators at time equal zero, which we will write them simply J_l from now on, and c_Θ and s_Θ are the trigonometric functions introduced on the first chapter.

We need to compute the second and the fourth moments of J_x as it is required by the Equation (3.2). But before any calculation we will make a simplifying assumption which turn to be well supported on the most common situations. The assumption is that both expectation values are even functions on Θ,

$$\begin{aligned} \langle J_x^2(\Theta) \rangle &= \langle J_x^2(-\Theta) \rangle, \\ \langle J_x^4(\Theta) \rangle &= \langle J_x^4(-\Theta) \rangle. \end{aligned} \tag{3.4}$$

The square of J_x in the Heisenberg picture is written as follows,

$$J_x^2(\Theta) = J_x^2 \mathrm{c}_\Theta^2 + J_y^2 \mathrm{s}_\Theta^2 - (J_x J_y + J_y J_x)\mathrm{c}_\Theta \mathrm{s}_\Theta. \tag{3.5}$$

From the equation above and to fulfill the first constraint on the Equation (3.4) it turns out that the

expectation value over our yet to be shown initial state of the operator $(J_xJ_y + J_yJ_x)$ must vanish. Hence it is equivalent to the first assumption of the Equation (3.4) write that

$$\langle \{J_x, J_y\} \rangle = 0 \tag{3.6}$$

where $\{\ ,\ \}$ stands for the anticommutator. Apart for been simpler to compute the Equation (3.6) is based also on initial expectation values of the state. We will see that as we said before this is easily guarantied for most important cases.

As we have done recently with the square of J_x now we will do it for J_x^4. This way one will be able to distinguish which other combination of operators must vanish in order to have Equation (3.4) guarantied. The fourth power of J_x can be written as follows in the Heisenberg picture,

$$\begin{aligned} J_x^4(\Theta) = J_x^4 c_\Theta^4 + J_y^4 s_\Theta^4 + (J_x^2J_y^2 + J_xJ_yJ_xJ_y + J_xJ_y^2J_x + J_yJ_xJ_yJ_x + J_yJ_x^2J_y + J_y^2J_x^2)c_\Theta^2 s_\Theta^2 \\ - (J_x^3J_y + J_x^2J_yJ_x + J_xJ_yJ_x^2 + J_yJ_x^3)c_\Theta^3 s_\Theta - (J_xJ_y^3 + J_yJ_xJ_y^2 + J_y^2J_xJ_y + J_y^3J_x)c_\Theta s_\Theta^3. \end{aligned} \tag{3.7}$$

And again assuming that its expectation value must be an even function on Θ it turns out that the second line must be equal to zero when the expectation value is considered. So $(J_x^3J_y + J_x^2J_yJ_x + J_xJ_yJ_x^2 + J_yJ_x^3)$ and $(J_xJ_y^3 + J_yJ_xJ_y^2 + J_y^2J_xJ_y + J_y^3J_x)$ must vanish again over any candidate state to be used as prove state. Hence, the second constraint of the Equation (3.4) can be rewritten as follows,

$$\begin{aligned} \langle \{J_x^2, \{J_x, J_y\}\} \rangle = 0, \\ \langle \{J_y^2, \{J_x, J_y\}\} \rangle = 0. \end{aligned} \tag{3.8}$$

Finally, we can write how the evolution of second and fourth moments of the J_x operator must look like,

$$\langle J_x^2(\Theta) \rangle = \langle J_x^2 \rangle c_\Theta^2 + \langle J_y^2 \rangle s_\Theta^2 \tag{3.9}$$

$$\begin{aligned} \langle J_x^4(\Theta) \rangle = \langle J_x^4 \rangle c_\Theta^4 + \langle J_y^4 \rangle s_\Theta^4 \\ + \langle \{J_x^2, J_y^2\} + \{J_x, J_y\}^2 \rangle c_\Theta^2 s_\Theta^2. \end{aligned} \tag{3.10}$$

From here we are able to write the evolution of the variance of the second moment when Equation (3.4)

must be obeyed. We obtain

$$\begin{aligned}(\Delta J_x^2(\Theta))^2 &= \langle J_x^4(\Theta)\rangle - \langle J_x^2(\Theta)\rangle^2 \\ &= \langle J_x^4\rangle c_\Theta^4 + \langle J_y^4\rangle s_\Theta^4 + \langle\{J_x^2, J_y^2\} + \{J_x, J_y\}^2\rangle c_\Theta^2 s_\Theta^2 - \left(\langle J_x^2\rangle c_\Theta^2 + \langle J_y^2\rangle s_\Theta^2\right)^2 \\ &= \left(\langle J_x^4\rangle - \langle J_x^2\rangle^2\right)c_\Theta^4 + \left(\langle J_y^4\rangle - \langle J_y^2\rangle^2\right)s_\Theta^4 + \left(\langle\{J_x^2, J_y^2\} + \{J_x, J_y\}^2\rangle - 2\langle J_x^2\rangle\langle J_y^2\rangle\right)c_\Theta^2 s_\Theta^2 \\ &= (\Delta J_x^2)^2 c_\Theta^4 + (\Delta J_y^2)^2 s_\Theta^4 + \left(\langle\{J_x^2, J_y^2\} + \{J_x, J_y\}^2\rangle - 2\langle J_x^2\rangle\langle J_y^2\rangle\right)c_\Theta^2 s_\Theta^2.\end{aligned} \tag{3.11}$$

The remaining constituent of the Equation (3.2) on which we will base our result for the precision, is the modulus square of the derivative of the second moment of the J_x operator. Using Equation (3.9) for the expression of the evolution of the second moment, the denominator of Equation (3.2) follows

$$\begin{aligned}|\partial_\Theta\langle J_x^2(\Theta)\rangle|^2 &= |-2\langle J_x^2\rangle c_\Theta s_\Theta + 2\langle J_y^2\rangle c_\Theta s_\Theta|^2 \\ &= 4\langle J_y^2 - J_x^2\rangle^2 c_\Theta^2 s_\Theta^2.\end{aligned} \tag{3.12}$$

From the equations above directly follows expression for the precision of Θ,

$$\begin{aligned}(\Delta\Theta)^2 &= \frac{(\Delta J_x^2)^2 c_\Theta^4 + (\Delta J_y^2)^2 s_\Theta^4 + \left(\langle\{J_x^2, J_y^2\} + \{J_x, J_y\}^2\rangle - 2\langle J_x^2\rangle\langle J_y^2\rangle\right)c_\Theta^2 s_\Theta^2}{4\langle J_y^2 - J_x^2\rangle^2 c_\Theta^2 s_\Theta^2} \\ &= \frac{(\Delta J_x^2)^2 t_\Theta^{-2} + (\Delta J_y^2)^2 t_\Theta^2 + \langle\{J_x^2, J_y^2\} + \{J_x, J_y\}^2\rangle - 2\langle J_x^2\rangle\langle J_y^2\rangle}{4\langle J_y^2 - J_x^2\rangle^2}.\end{aligned} \tag{3.13}$$

To this calculations further computations follows mainly regarding to the following expectation value $\langle\{J_x^2, J_y^2\} + \{J_x, J_y\}^2\rangle$. This calculus is left for the Appendix A.1. Finally, the expression Equation (3.13) leads to the following,

$$(\Delta\Theta)^2 = \frac{(\Delta J_x^2)^2 t_\Theta^{-2} + (\Delta J_y^2)^2 t_\Theta^2 + 4\langle J_y^2\rangle - 3\langle J_z^2\rangle - 2\langle J_x^2\rangle(1 + \langle J_y^2\rangle) + 6\langle J_x J_y^2 J_x\rangle}{4\langle J_y^2 - J_x^2\rangle^2} \tag{3.14}$$

[WOW IN THE PAPER FINALLY IT IS CORRECT!!]

We have verified the correctness of our analytical formula with a direct numeric simulation of the Equation [ERROR PROP. FORM.] and the equation above. For that we, have used the ground-state of $H = J_x^2 + J_y$ for 6 qubits, $|GS\rangle$. This state in principle does not have extra symmetries where further simplifications would take part on the final expression of the formula, so is more adequate for testing. We have computed the evolution of the expectation values of the second and the fourth moments of the operator J_x in the range of half a cycle, *i.e.*, $\Theta \in [0, \pi]$, for thousand of equidistant points. We choose so high density of points on the range in order to compute a more accurate derivative of the

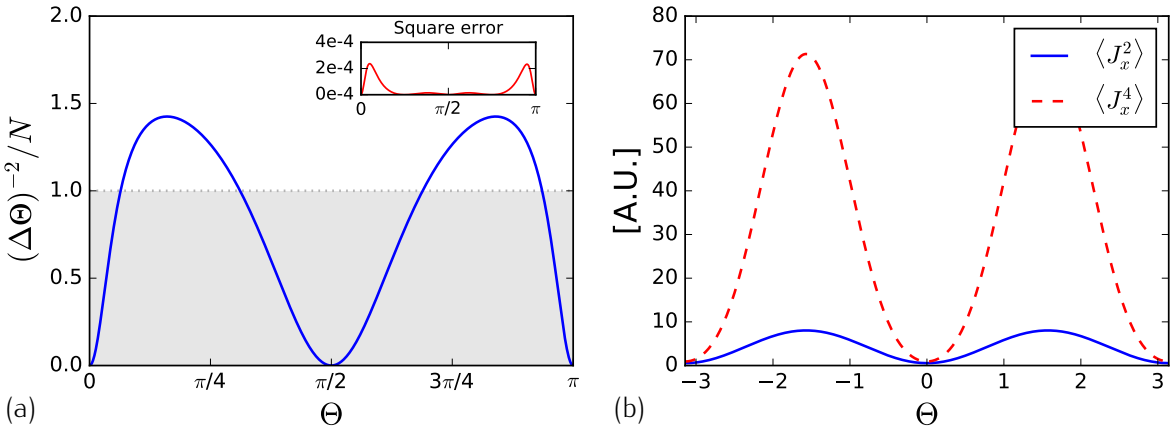

Figure 3.2: (a) Evolution of the precision for 6 qubits based on the simulation of the system and its expectation values. The agreement with the Equation [REF] is shown on the inset plot where the square of the difference between two approaches, the analytical and the simulation, is plotted. The difference is more or less two orders of magnitude below the actual value for the relevant points, which mainly comes because of the error coming from computing the derivative which has to be done approximately between two neighbor points. (b) Verification of the parity with respect to Θ of the expectation values of the second and the fourth moment, so to fulfill the constraint Equation [REF].

expectation value $\partial_\Theta \langle J_x^2 \rangle$ appearing on the Equation [EPF], see Figure [REF] (a). Finally, we have also checked that the constraints assumed at the beginning of this section are fulfilled. For that aim, the range of the evolution time has been $\Theta \in [-\pi, \pi]$ and we have computed the expectation values for five hundreds of equidistant points, see Figure [REF] (b). We can conclude saying that our formula exactly reproduces the evolution of the error propagation formula, Equation [REF].

3.2.1 The optimal precision

One can realize that the whole dependence on the phase shift is in the first two terms of the numerator. This way one can minimize the sum on the first two terms in order to find where the precision is best. So it follows that,

$$\tan^2(\Theta_{\text{opt}}) = \sqrt{\frac{(\Delta J_x^2)^2}{(\Delta J_y^2)^2}} \tag{3.15}$$

which inserted on the Equation (3.14) gives us the optimal precision when the second moment $\langle J_x^2 \rangle$ is measured based on the initial expectation values of the input state. The optimal precision is written in the following way,

$$(\Delta\Theta)^2_{\text{opt}} = \frac{\sqrt{(\Delta J_x^2)^2(\Delta J_y^2)^2} + 4\langle J_y^2 \rangle - 3\langle J_z^2 \rangle - 2\langle J_x^2 \rangle(1 + \langle J_y^2 \rangle) + 6\langle J_x J_y^2 J_x \rangle}{4\langle J_y^2 - J_x^2 \rangle^2}. \tag{3.16}$$

.

We conclude with this section checking our bound for the pure unpolarised Dicke state aligned with Ox, $|D_N\rangle_x$, whose precision bound is well known, Equation ([XXX]). With this aim we compute all the expectation values needed for the Equation (3.16) which almost all of them are trivial, $\langle J_x J_y^2 J_x\rangle = \langle J_x^4\rangle = \langle J_x^2\rangle = 0$. The rest are obtained in the following way,

$$\langle J_y^2\rangle = \langle J_z^2\rangle = \frac{N(N+2)}{8}, \tag{3.17}$$

$$\langle J_y^4\rangle = \frac{N+2}{8}\left(\frac{3N(N+2)}{16} - \frac{1}{2}\right). \tag{3.18}$$

The Equation (3.17) follows directly from the fact that the state is invariant under rotations on the Ox axis, so they are its expectation values, because the sum of all the second moments must give the value of the total angular momentum, in this case the maximum which is $\langle \boldsymbol{J}^2\rangle = \frac{N(N+2)}{4}$, and because $\langle J_x^2\rangle = 0$. The proof of the Equation (3.18) needs more algebra and has been left for the Appendix **??**.

From the equations above, one lead to the following expression for the precision of the phase shift for a pure unpolarised Dicke state,

$$(\Delta\Theta)^2 = \frac{2}{N(N+2)}, \tag{3.19}$$

which coincides exactly with the inverse quantum Fisher information for such state.

3.3 Testing the formula against some known states

In this section we will compare our criteria based on few expectation values against the corresponding quantum Fisher information obtained for some known input states. Those input states will be first the family of states defined as the ground states of the following Hamiltonian, called the spin-squeezing Hamiltonian,

$$H_\lambda = J_x^2 - \lambda J_y. \tag{3.20}$$

For λ equal to zero we have the unpolarized Dicke state, Equation (3.1), and for λ large we recover the coherent totally polarized state pointing onto the Oy direction. In the meantime the state is also a spin-squeezed state, therefore the name of the Hamiltonian. The ground state is defined such that

$$\lambda_{\min} = \mathrm{tr}(H_\lambda \rho_\lambda), \tag{3.21}$$

where $\lambda_{\min}$ is the lowest eigenvalue of H_λ. The state ρ_λ is invariant under permutations of the particles and it is also pure. Moreover the state ρ_λ is symmetric.

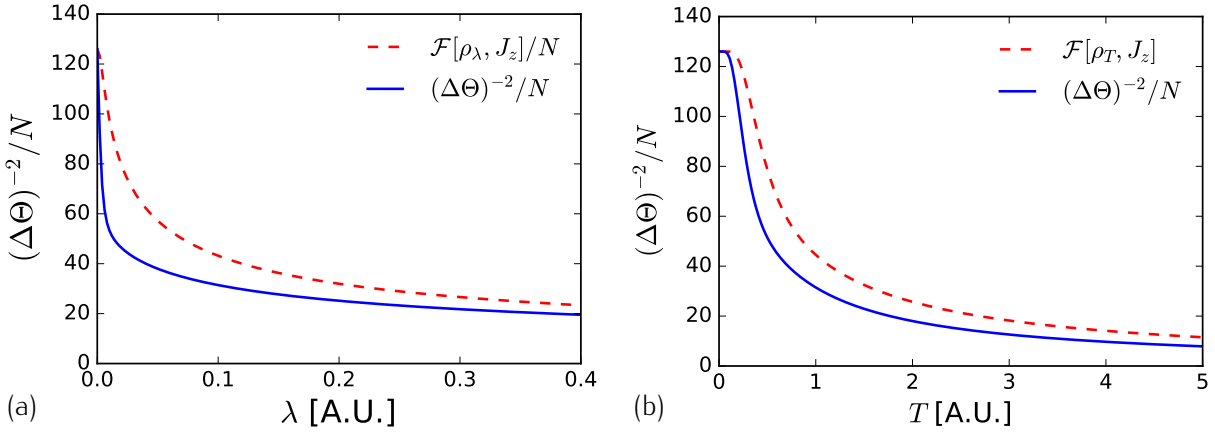

Figure 3.3: Comparison between our formula for the precision and the QFI for different states. (a) Comparison for ground states of H_λ. (b) Comparison with gaussian mixture of Dicke states.

The second family of input states we are going use are the Gaussian mixture of Dicke states around the unpolarized Dicke state, which have the following form as function of β,

$$\rho_{(T)} \propto \sum_{m=-N/2}^{N/2} e^{-\frac{m^2}{T}} |\mathrm{D}_N^m\rangle_x\langle \mathrm{D}_N^m|_x. \tag{3.22}$$

After showing how the optimal precision formula behaves compared with the quantum Fisher information for those two families of states, we also have to proof that they indeed fulfill the constraints on Equation (3.4).

For the spin-squeezed state , ρ_λ, we have that it is invariant under

On the other hand for the thermal state, ρ_T, we have that it is invariant under rotations around the Ox axis

$$\rho_T = e^{-i\alpha J_x}\rho_T e^{i\alpha J_x}, \tag{3.23}$$

for arbitrary $\forall\alpha$.

$$\mathrm{tr}(e^{i\Theta J_z}J_y^m e^{-i\Theta J_z}\rho_T) = \mathrm{tr}(e^{i\Theta J_z}J_y^m e^{-i\Theta J_z}e^{-i\alpha J_x}\rho_T e^{i\alpha J_x}) \tag{3.24}$$

If we choose $\alpha = \pi$ then we rotate all the orthogonal angular momentum operators such that $J_y \to -J_x$ and $J_z \to -J_z$. Therefore, $e^{i\pi J_x}e^{i\Theta J_z}J_y^m e^{-i\Theta J_z}e^{-i\pi J_x} = e^{-i\Theta J_z}(-J_y)^m e^{i\Theta J_z}$. Hence, for even m and particularly for $m = 2, 4$ we have that,

$$\mathrm{tr}(e^{i\Theta J_z}J_y^m e^{-i\Theta J_z}\rho_T) = \mathrm{tr}(e^{-i\Theta J_z}J_y^m e^{i\Theta J_z}\rho_T), \tag{3.25}$$

so the Equation (XXX) is granted.

3.4 Using our method with real experimental data

On reference [XXX], it is produced on the laboratory a state with the proper characteristics of an unpolarised Dicke state, small variance on one of the directions and very large one on the perpendicular directions to this. It is also invariant under rotations around Ox-axis. Effectively, the state has the following form,

$$\rho = \frac{1}{2\pi}\int e^{-i\alpha J_x}\rho_0 e^{i\alpha J_x}, \tag{3.26}$$

where $\rho_0$is what we would obtain if we would have access to the phase reference. Hence we have that at $\Theta = 0$ all the statistical moments $\langle J_z^m\rangle = \langle J_y^m\rangle$ are equal.

Simplification of our precision formula on Equation (XXX). First, we simplify the expectation value $\langle J_x J_z^2 J_x\rangle$ in the following way,

$$\begin{aligned}\langle J_x J_y^2 J_x\rangle &= \frac{\langle J_x(J_y^2+J_z^2)J_x\rangle}{2} = \frac{\langle J_x(J_x^2+J_y^2+J_z^2)J_x\rangle - \langle J_x^4\rangle}{2}\\ &\leq \frac{N(N+2)}{8}\langle J_x^2\rangle - \frac{\langle J_x^4\rangle}{2}.\end{aligned} \tag{3.27}$$

Notice that obtaining $\langle J_x J_z^2 J_x\rangle$ is hard experimentally. This simplification can only make our estimation of the precision worse while for symmetric states the equality holds. The bound from below for the precision can be writtes as,

$$(\Delta\Theta)^2_{\text{opt}} \leq \frac{\sqrt{(\Delta J_x^2)^2(\Delta J_y^2)^2} + \langle J_y^2\rangle + \frac{3N(N+2)-8}{4}\langle J_x^2\rangle - 2\langle J_x^2\rangle\langle J_y^2\rangle - 3\langle J_x^4\rangle}{4\langle J_y^2 - J_x^2\rangle^2}, \tag{3.28}$$

where some terms were reordered and further simplified.

It is worth to study this case and apply our methods such that we can extract conclusions about the metrological usefulness of the state. The system in consideration is a $N = 7900$ particles system. The measured data for such system is

$$\begin{aligned}\langle J_x^2\rangle &= 112 \pm 31, & \langle J_y^2\rangle &= 6\times 10^6 \pm 0.6\times 10^6,\\ \langle J_x^4\rangle &= 40\times 10^3 \pm 22\times 10^3, & \langle J_y^4\rangle &= 6.2\times 10^{13} \pm 0.8\times 10^{13}.\end{aligned} \tag{3.29}$$

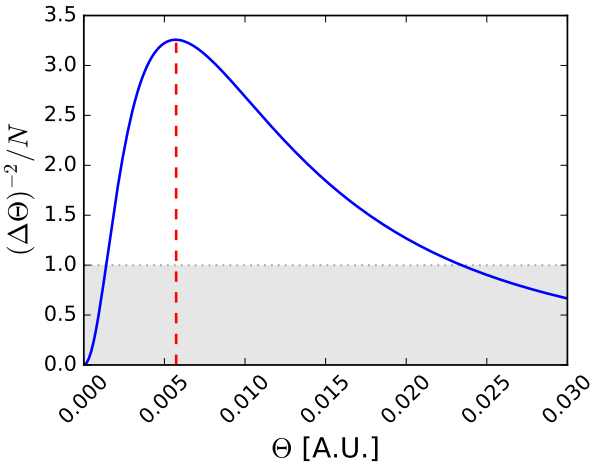

Figure 3.4: The (solid) line shows how the precision of Θ varies through the evolution. Notice that for the initial moment the precision is zero and that it reaches a maximum at $\Theta \approx 0.0057$ highlighted with the vertical (dashed) line. The gray area represent the region where the precision is below the shot-noise limit.

Hence we obtain the maximum precision,

$$\frac{(\Delta\Theta)^{-2}_{\text{opt}}}{N} \geq 3.7 \pm 1.5 \tag{3.30}$$

with boot straping methods. The direct substitution would yield to a 3.3 gain over the shot-noise limit.

Next we plot the value for the precision substituting directly the measured data into Equation (XXX), see Figure 3.4.

Further simplification of our method can be achieved for states of the kind of the one studied on this section. Based on $\langle AB\rangle \leq \lambda_{\text{max}}(A)\langle B\rangle$ for two commuting positive-semidefinite observables,

$$\langle J_y^4\rangle \leq \frac{N^2}{4}\langle J_x^2\rangle. \tag{3.31}$$

We can also approximate $\langle J_x^4\rangle$ with $\langle J_x^2\rangle$ in the sense that it is small and that mainly its value comes from technical noise,

$$\langle J_x^4\rangle \approx \beta\langle J_x^2\rangle^2. \tag{3.32}$$

This approximation even if it is not a strict bound on the precision can be very useful in order to characterize the metrological usefulness of our input state based only on second statistical moments of only two angular momentum operators, namely $\langle J_z^2\rangle$ and $\langle J_x^2\rangle$. Those two expectation values are

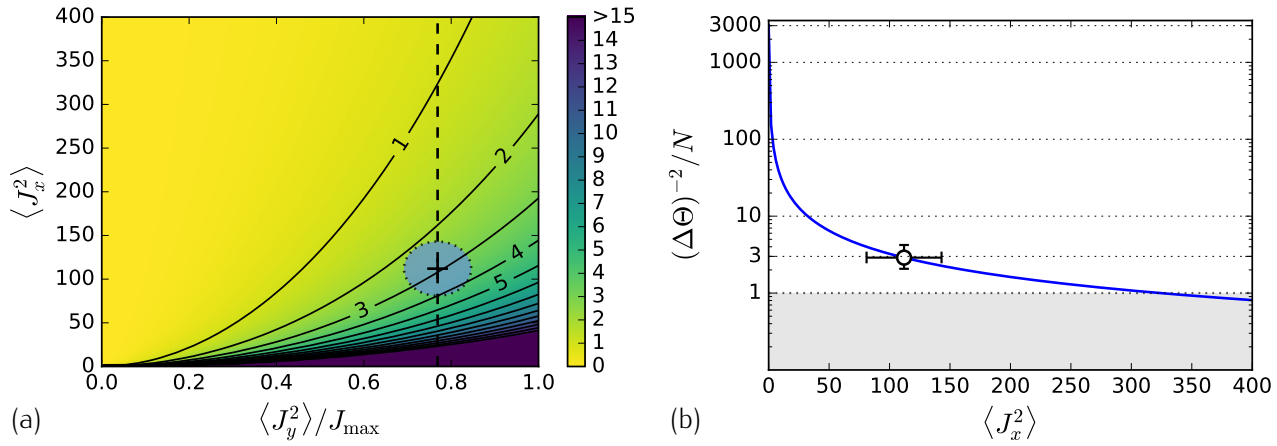

Figure 3.5: Comparison between our formula for the precision and the QFI for different states. a) Comparison for ground states of H_λ. (b) Comparison with gaussian mixture of Dicke states.

related with the width of our state and also with how thin we can do it in one of the directions, for metrological purposes, perpendicular to the magnetic field. So in this case we use $\beta = 3$ assuming that the distribution function has Gaussian shape.

From these considerations we are able to write a second bound with fewer expectation values for the optimal precision such that,

$$(\Delta\Theta)^2_{\text{opt}} \leq \frac{\langle J_y^2 \rangle + \frac{3N(N+2)-8}{4}\langle J_x^2 \rangle + \left(\sqrt{\frac{N^2}{2\langle J_y^2 \rangle} - 2} - 2\right)\langle J_y^2 \rangle \langle J_x^2 \rangle - 9\langle J_x^2 \rangle^2}{4\langle J_y^2 - J_x^2 \rangle^2}. \tag{3.33}$$

We have used this formula to compute the bound on the optimal precision with the measured data shown on Equation (XXX), $(\Delta\Theta)^{-2}_{\text{opt}} \geq 2.9N$, see Figure 3.5.

4 Witnessing metrologically useful entanglement

Typically, one has not access to the density matrix of the system been used for metrology or for other quantum process. Moreover, for systems on which the particle number is very large, this is the case when one wants to do metrology with quantum states, the details of the density matrix are forbidden by practical reasons. Since the quantum Fisher information is based on the complete knowledge of the density matrix, shortcuts to avoid the complete tomography must be developed as we have had shown one practical case on the previous chapter. In this chapter, we obtain a general procedure to get an optimal bound for the quantum Fisher information based on as many expectation values of the initial state as one is ready to measure. Two main features are worth to mention again. First, in general this method gives us an optimal tight bound. Last but not least, the bound is based on the expectation values of the initial state only, so it is not necessary to perform an evolution of the state to estimate how well will it behave. This is in contrast to other approaches one can find in the literature, an it is a time saving concept.

The figure of merit of bounds from below for the quantum Fisher information based on expectation

values of the initial state is the following,

$$\mathcal{F}_{\mathrm{Q}}[\rho, J_z] \geq \frac{\langle J_x \rangle^2}{(\Delta J_y)^2}. \tag{4.1}$$

where the state is polarized along the Ox-axis and the variance of the J_y operator is smaller than the standard. On the previous chapter we also have shown one of these bound specifically designed for unpolarized Dicke states.

Homogeneous magnetometry, $\boldsymbol{B} = B\boldsymbol{k}$ where B is constant in time.

Section [REF], see magnetometry, generator J_z.

Quantum Fisher information $\mathcal{F}_{\mathrm{Q}}[\rho, J_z]$.

4.1 Minimum of a convex function of the state given some expectation values

Convex function of state, $g(\rho)$.

Which is the lowest possible value of $g(\rho)$ for a state where some expectation values of $\{W_i\}_{i=1}^M$ operators, $w_i = \mathrm{tr}(\rho W_i)$ are known?

Such bound is defined in a way to fulfill the following inequality,

$$g(\rho) \geq \mathcal{B}_g(w_1, w_2, \ldots) := \left\{ \min_{\rho} g(\rho) \,|\, \{w_i = \mathrm{tr}(\rho W_i)\}_{i=1}^M \right\}. \tag{4.2}$$

When computing this bound we will require to this to be as tight as possible.

For this purpose we simplify our discourse to one expectation value and therefore one observable, $w = \mathrm{tr}(\rho W)$. Later we will extend our results to the multi-parameter case.

Notice that the tightest bound from below on of such a function $g(\rho)$ is convex too on the expectation values, *i.e.*, $\mathcal{B}_g(w)$ is convex if $g(\rho)$ is convex. This is shown in the following way,

Therefore, theory tells us that we can use the Legendre transform to get rid of the state preserving all the necessary information to reconstruct the $\mathcal{B}_g$ bound from the expectation values, this can be found on the work of Prof. Gühne and Prof. Werner Reference [?] and for a brief description of the properties of the Legendre transform see Appendix ??. In this case the Legendre transform can be written in the following way,

$$\hat{g}(rW) = \sup_{\rho} \{ r\langle W \rangle_\rho - g(\rho) \}. \tag{4.3}$$

Now we have the Legendre transform, we recover the bound from below of $g(\rho)$ as

$$\mathcal{B}_g(w) = \sup_r \left\{ rw - \sup_\rho \{ r\langle W\rangle_\rho - g(\rho)\}\right\}. \tag{4.4}$$

To clarify, notice that the ρ appearing on the inner maximization is not related with the one appearing on $g(\rho)$ that is bounded by $\mathcal{B}_g$ but a variable state for the maximization.

The Equation (4.4) has been applied on entanglement measures, when $g(\rho)$ is defined using the convex roof construction, *i.e.*, the function $g(\rho)$ is extended from the well defined region, namely the region of pure states, to the mixed states using the convex roof construction. For illustrative purposes the convex roof of a function defined for pure states is the following,

$$g(\rho) = \inf_{\{p_k, |\phi_k\rangle\}} \Big\{ \sum_k p_k g(|\phi_k\rangle)\Big\} \tag{4.5}$$

for any decomposition $\rho = \sum_k p_k |\phi_k\rangle\langle\phi_k|$ In this case the Equation (4.4) can be further simplified. Let us focus by now on the inner maximization,

$$\begin{aligned}
\hat{g}(rW) &= \sup_\rho \{ r\langle W\rangle_\rho - g(\rho)\} \\
&= \sup_\rho \left\{ r\langle W\rangle_\rho - \inf_{\{p_k, |\phi_k\rangle\}} \Big\{ \sum_k p_k g(|\phi_k\rangle)\Big\}\right\} \\
&= \sup_{\{p_k, |\phi_k\rangle\}} \left\{ \sum_k p_k r\langle W\rangle_{|\phi_k\rangle} - \inf_{\{p_k, |\phi_k\rangle\}} \Big\{ \sum_k p_k g(|\phi_k\rangle)\Big\}\right\} \\
&= \sup_{\{p_k, |\phi_k\rangle\}} \left\{ \sum_k p_k \big\{ r\langle W\rangle_{|\phi_k\rangle} - g(|\phi_k\rangle)\big\}\right\} \\
&= \sup_{|\psi\rangle} \big\{ r\langle W\rangle_{|\psi\rangle} - g(|\psi\rangle)\big\}.
\end{aligned} \tag{4.6}$$

So now we have restricted the maximization to only pure states as it is shown on Reference [?].

One the other hand, one can find different definitions of the QFI in the literature. Among those definitions, there is one that defines the QFI as the convex roof of four times the variance of the generator of the unitary phase shift that suffers the state [?]. This can be written in the following way,

$$\mathcal{F}_Q[\rho, G] = \inf_{\{p_k, |\phi_k\rangle\}} 4 \sum_k p_k (\Delta G)^2_{|\phi_k\rangle} \tag{4.7}$$

Even further simplification can be achieved for quantum Fisher information,

$$\begin{aligned}\hat{\mathcal{F}}_{\mathrm{Q}}(rW) &= \sup_{|\psi\rangle}\left\{r\langle W\rangle_{|\psi\rangle} - 4(\Delta J_z)^2_{|\psi\rangle}\right\} \\ &= \sup_{|\psi\rangle}\left\{r\langle W\rangle_{|\psi\rangle} - 4\langle J_z^2\rangle_{|\psi\rangle} + 4\langle J_z\rangle^2_{|\psi\rangle}\right\} \\ &= \sup_{|\psi\rangle}\{\langle rW - 4J_z^2\rangle_{|\psi\rangle} + \langle 2J_z\rangle^2_{|\psi\rangle}\},\end{aligned} \tag{4.8}$$

which is clearly a second order maximization over pure states.

With that at hand we are able to prove the following observation: the Legendre transform of the highest lower bound of the quantum Fisher information when the expectation value of some operator W is known, can be written as the maximization over some parameter μ of the highest eigenvalue $\lambda_{\max}(rW - 4(J_z - \mu)^2)$. This can be expressed as follows,

$$\hat{\mathcal{F}}_{\mathrm{Q}}(rW) = \sup_{\mu}\{\lambda_{\max}(rW - 4(J_z - \mu)^2)\}, \tag{4.9}$$

where at the maximum the derivative with respect to μ must be zero for this quadratic function on the state. Hence, the value of μ will coincide with the expectation value on the optimal state $\langle J_z\rangle_\psi$ Therefore, the finding of the optimal parameter μ is delimited to the range defined by $[\langle J_z\rangle_{\min}, \langle J_z\rangle_{\max}]$. For qubits this means that we have to perform a search for μ_{opt} in between $-N/2 \leq \mu \leq N/2$.

Another way of getting the result of the maximization for the second order equation is parameterizing the eigenstate with the maximum eigenvalue of the operator $rW - 4(J_z - \mu)^2$, so we get $|\phi_{\max}(\mu)\rangle$, and finally computing the expectation values of Equation (4.8) and maximizing it.

With this a tight bound from below for the quantum Fisher information can be found when the expectation value of an observable, say W, is known as follows,

$$\mathcal{B}_{\mathcal{F}}(w) = \sup_{r}\left\{rw - \sup_{|\psi\rangle}\{\langle rW - 4J_z^2\rangle + \langle 2J_z\rangle^2\}\right\}. \tag{4.10}$$

One may notice that the inner maximization is a second order maximization.

This can be extended for several observables as follows

$$\mathcal{B}_{\mathcal{F}}(w_1, w_2, \ldots) = \sup_{\boldsymbol{r}}\left\{\boldsymbol{rw} - \sup_{|\psi\rangle}\{\langle \boldsymbol{rW} - 4J_z^2\rangle + \langle 2J_z\rangle^2\}\right\}, \tag{4.11}$$

where $\boldsymbol{r} = (r_1, \ldots, r_m)$ is the vector form and the same applies to $\boldsymbol{w}$ and the operators set $\boldsymbol{W}$. The contraction of two of those vectors must be seen as a scalar product, *i.e.*, $\boldsymbol{rW} = \sum r_i W_i$ where W_i is

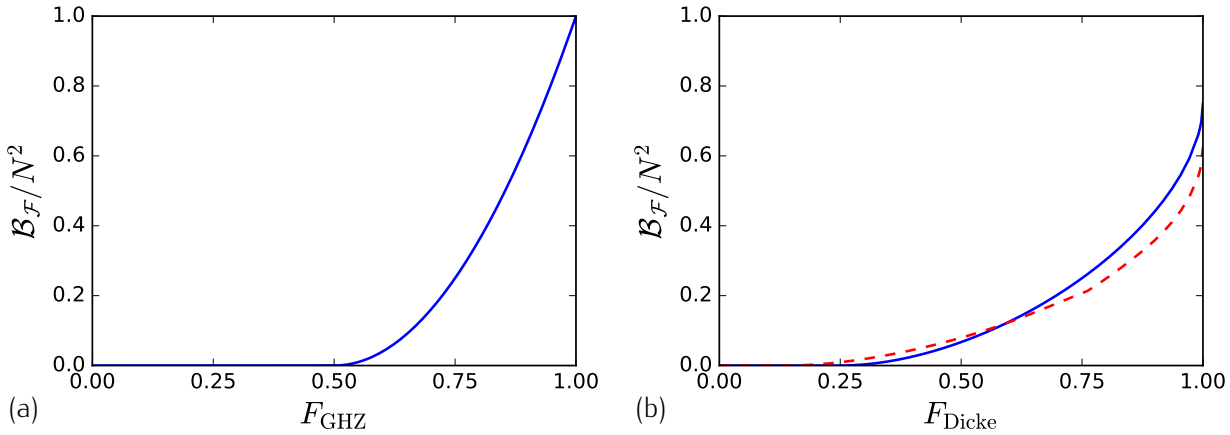

Figure 4.1: (a) Analytical solution of the bound $\mathcal{B}_\mathcal{F}$ for different values of the fidelity with respect to the GHZ state. (b) Numerical results for the minimum quantum Fisher information as a function of the fidelity with respect of unpolarise Dicke states perpendicular to the magnetic field, $|\mathrm{D}_N^0\rangle$. (blue-line) For systems with 4 particles and (red-dashed) for system with 8 particles. One may notice that when the fidelity is at its maximum the bound approaches to 0.5 as it is the quantum Fisher information for large particle number.

the corresponding i^{th} operator of $\boldsymbol{W}$.

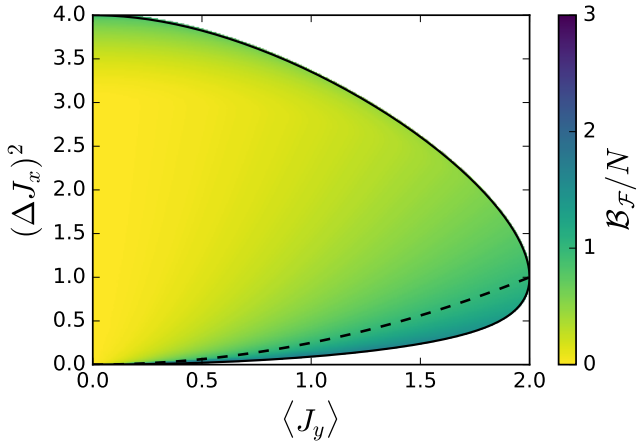

Figure 4.2: (dashed) Boundary for the SQL, all points above the line achieve semi-classical precisions, while the points below the line achieve better precisions than with classical systems.

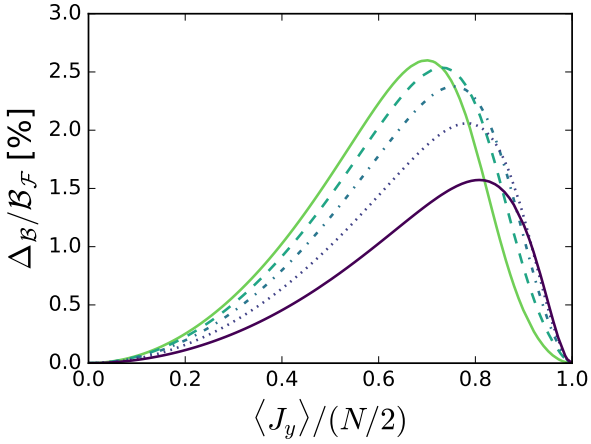

Figure 4.3: Difference between the bound of Pezze-Smerzi and the optimal bound for the quantum Fisher information normalized by the value of the optimal bound itself for the bosonic ground states of $H = J_x^2 - \lambda J_y$ for $\forall \lambda \in [0, \infty)$. From dark to lighter colors (line, point, dash-point, dashed, pointed, line), results for different particle numbers, $N = 4, 6, 10, 20, 1000$ respectively. Heuristically speaking, one can say that for large particle number the difference is biggest when the polarisation is around two thirds of the maximal polarisation and that this difference is about 2.6%.

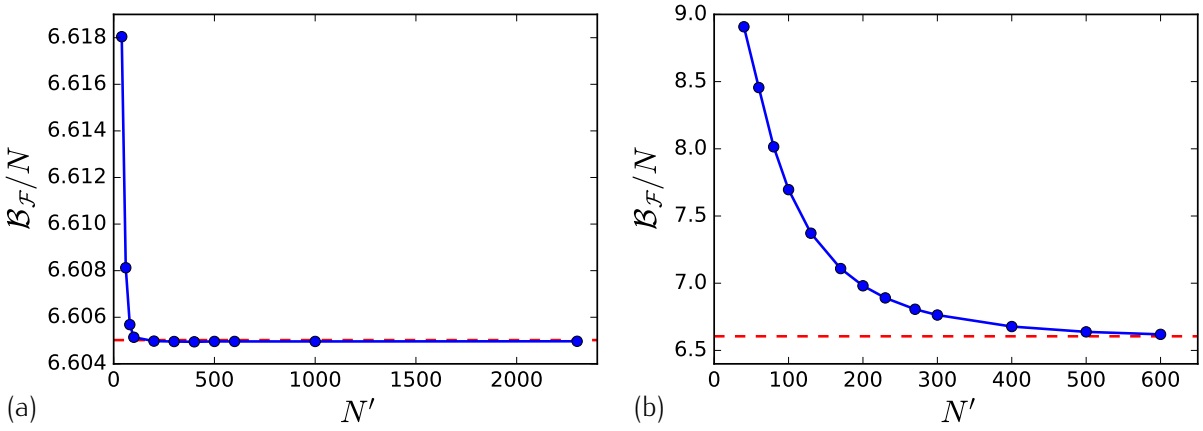

Figure 4.4

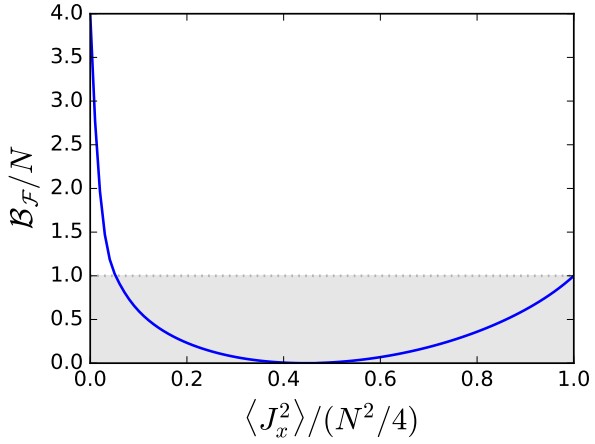

Figure 4.5: The numerics shows us a tiny region the symmetric system surpassing the shot-noise threshold.

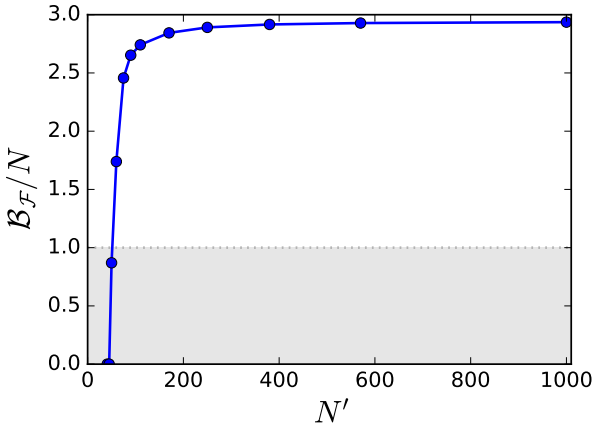

Figure 4.6: Secuence of the evolution of an unpolarized Dicke state of 16 qubits for $\Theta = \{i\pi/6\}_{i=0}^{4}$. Bloch spheres representing the Hirusi distribution of the state, and below PDF of the J_x POVM for each step of the secuence

5 Accuracy bound for gradient field estimation with atomic ensembles

$$\mathcal{F}_Q \tag{5.1}$$

6 Conclusions

Hello it's me again

A. Long calculus appearing through the sections

In this appendix we will develop long calculations appeared throughout different chapters.

A.1 Simplification of $\langle \{J_x^2, J_y^2\} + \{J_x, J_y\}^2 \rangle$

The expectation value appearing on Equation (3.13) which we want to simplify has 6 different terms, all with two J_x and another two J_y,

$$\langle J_x^2 J_y^2 \rangle + \langle J_x J_y J_x J_y \rangle + \langle J_x J_y^2 J_x \rangle + \langle J_y J_x^2 J_y \rangle + \langle J_y J_x J_y J_x \rangle + \langle J_y^2 J_x^2 \rangle. \tag{A.1}$$

From all those terms the third is somehow referent, since the pure unpolarised Dicke state used as reference is align with the Ox-axis, so $J_x |D_N^{N/2}\rangle_x = 0$.

We use the commutation relations of the angular momentum operators $[J_k, J_l] = \epsilon_{klm} i J_m$ to rearrange

all operators,

$$\langle J_x^2 J_y^2\rangle = i\langle J_x J_z J_y\rangle + \langle J_x J_y J_x J_y\rangle, \tag{A.2a}$$
$$\langle J_x J_y J_x J_y\rangle = i\langle J_x J_y J_z\rangle + \langle J_x J_y^2 J_x\rangle, \tag{A.2b}$$
$$\langle J_x J_y^2 J_x\rangle = \langle J_x J_y^2 J_x\rangle, \tag{A.2c}$$
$$\langle J_y J_x^2 J_y\rangle = i\langle J_y J_x J_z\rangle + \langle J_y J_x J_y J_x\rangle, \tag{A.2d}$$
$$\langle J_y J_x J_y J_x\rangle = -i\langle J_z J_y J_x\rangle + \langle J_x J_y^2 J_x\rangle, \tag{A.2e}$$
$$\langle J_y^2 J_x^2\rangle = -i\langle J_y J_z J_x\rangle + \langle J_y J_x J_y J_x\rangle. \tag{A.2f}$$

One may notice that with those relations is enough to see that we have six $\langle J_x J_y^2 J_x\rangle$, for instance, Equation (A.2a) is $i\langle J_x J_z J_y\rangle$ plus Equation (A.2b) which at the same time is $i\langle J_x J_y J_z\rangle$ plus Equation (A.3c). So each equation has at the end one $\langle J_x J_y^2 J_x\rangle$ plus or minus some expectation value of the product of three operators.

For the three terms operators and again using the commutation relations we can further simplify this expression. Trying to get one $\langle J_x J_y J_z\rangle$ on each term, we obtain the following,

$$i\langle J_x J_z J_y\rangle = \langle J_x^2\rangle + i\langle J_x J_y J_z\rangle, \tag{A.3a}$$
$$2i\langle J_x J_y J_z\rangle = 2i\langle J_x J_y J_z\rangle, \tag{A.3b}$$
$$i\langle J_y J_x J_z\rangle = \langle J_z^2\rangle + i\langle J_x J_y J_z\rangle, \tag{A.3c}$$
$$-i\langle J_y J_z J_x\rangle = \langle J_y^2\rangle - \langle J_z\rangle - i\langle J_x J_y J_z\rangle \tag{A.3d}$$
$$\begin{aligned} -3i\langle J_z J_y J_x\rangle &= -3\langle J_x^2\rangle - 3i\langle J_y J_z J_x\rangle \\ &= -3\langle J_x^2\rangle + 3\langle J_y^2\rangle - 3i\langle J_y J_x J_z\rangle \\ &, = -3\langle J_x^2\rangle + 3\langle J_y^2\rangle - 3\langle J_z^2\rangle - 3i\langle J_x J_y J_z\rangle. \end{aligned} \tag{A.3e}$$

Now if we sum it all, note that the all 3 operators terms simplify, and if we take into account $6\langle J_x J_y^2 J_x\rangle$ the resulting expression is the following,

$$4\langle J_y^2\rangle - 3\langle J_z^2\rangle - 2\langle J_x^2\rangle + 6\langle J_x J_y^2 J_x\rangle \tag{A.4}$$

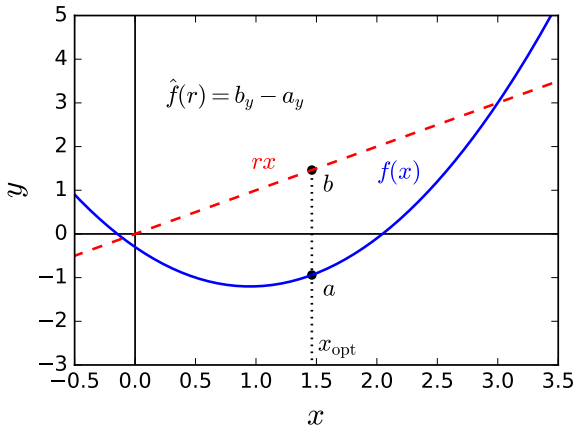

Figure A.1: Graphical representation of the Legendre transform. (blue-line) Convex function, $f(x) = x^2 - 1.9x - 0.3$, to be transformed. (red-dashed) Constant slope line passing by the coordinate system origin, rx. The Legendre transform is the maximal difference between rx and $f(x)$ at the same x. In this case, the vertical distance between a and b.

A.2 Legendre transform

The Legendre transform of a convex function, say $f : x \to f(x)$, is defined as the maximum distance between the function the line rx and $f(x)$ at same x. In can be written as follows,

$$\hat{f}(r) := \max_x \{rx - f(x)\}, \tag{A.5}$$

where $\hat{f}(r)$ represents the transformed function. A geometric representation of the transform is given on the Figure A.1.

The inverse transformation is simply obtained by applying again the same technique. One fully recovers the

$$f(x) = \max_r \{rx - \hat{f}(r)\}. \tag{A.6}$$

Let us develop the example shown in the Figure A.1, where the function is $f(x) = x^2 - 1.9x - 0.3$. In this case the problem is well defined on the complete real axis. Now, one has to find the maximum of $g(r, x) = rx - f(x)$ for all $\forall r$. This maximum is easily obtained in this particular case with usual techniques. On has to solve for x the following equation $\partial_x g(r, x) = 0$. Thus, the maximum is at $x_{\text{opt}} = \frac{r+1.9}{2}$ and hence, the Legendre transform is the following,

$$\hat{f}(r) = \frac{r^2}{4} + 0.95r + 1.2025. \tag{A.7}$$

If one applies again the transformation the resulting function is again the original one.

B. Miscellaneous mathematical tools

In this appendix we will illustrate basic mathematical tools used all through the thesis. They are shown here because without been figures of merit of the conceptual parts involving this thesis, they are nowadays sufficiently important for any whose intention is t expertise on this field of Quantum Metrology and Quantum Information.

B.1 Husimi Q-representation and the Bloch sphere

To represent states of total angular momentum bigger than $\frac{1}{2}$ we use the Husimi quasi-probability on the $\boldsymbol{n}$ unitary vector space defined as $2+2$

$$Q(\alpha) = \langle |\varrho| \alpha \rangle \tag{B.1}$$

where ...

It is very common to express the particle density.

B.2 Angular momentum subspaces for different spins

Here I want to show how the whole Hilbert space of the spin angular-momentum of a multi-particle system splits. There are severas constituents such as the symmetric subspace, the PI subspace, the anti-symmetric subspace, etc.

References